UDC 622.276.3
DOI: 10.15587/2706-5448.2025.329744

**Petro Molchanov,
Tetiana Surzhko,
Maksym Knysh,
Yuliya Sribna,
Vasyl Savyk,
Serhii Novopysmennyi,
Oleksii Debre,
Yuliia Salenko,
Serhii Hudz,
Dmytro Zakomirnyi**

MATHEMATICAL AND GRAPHICAL APPROACHES TO IMPROVE THE PROCESS OF SATURATION OF FLUSHING FLUID WITH AIR IN THE CIRCULATION SYSTEM OF A DRILLING RIG UNIT

The object of research is the process of air saturation of the flushing fluid using a multi-nozzle foam generator in the circulation systems of drilling rigs.

One of the most problematic areas in the known designs of foam generators is the insufficient efficiency of air saturation of the fluid, which is solved by the design proposed in the work. The design of a multi-nozzle foam generator is proposed by improving the mixing chamber. This design allowed to provide improved foam formation, more efficient air saturation of the flushing fluid, reduce the time of well development and increase the productivity of the device without changing the pressure and supply of fluid and air.

During the study, computer mathematical modeling was used (in the Maple 9.5 software environment), a study of the dependence of air flow on pressure and fluid flow at nozzle diameters of 4 mm and 6 mm was performed. The studies considered graphical analysis to determine the optimal operating modes of the foam generator.

An improved multi-nozzle foam generator with improved foaming efficiency, uniform saturation of the flushing fluid with air, reduced energy consumption and reduced well development time was obtained. This is due to the improvement of the design of the mixing chamber, which has a number of features. The proposed design provides intense turbulence, uniform mixing of the fluid with air, optimization of the geometric parameters of the nozzles and feed channels, as well as reduction of hydraulic losses in the foaming process.

Thanks to this research, it is possible to obtain indicators that characterize the pattern of increasing air flow in proportion to increasing pressure. Compared with known analogues, the proposed foam generator, thanks to the variable geometric parameters of the mixing chamber and nozzles, allows to obtain foam mixtures with a wider range of properties. Such geometric changes provide better saturation of the fluid with air, create more intense turbulence, reduce hydraulic losses, and also increase the productivity and efficiency of well development.

Keywords: *circulation system, cleaning unit, design, foam generator, mathematical modeling, software environment, graphical research.*

Received: 01.03.2025
Received in revised form: 17.04.2025
Accepted: 08.05.2025
Published: 19.05.2025

How to cite

Molchanov, P., Surzhko, T., Knysh, M., Sribna, Y., Savyk, V., Novopysmennyi, S., Debre, O., Salenko, Y., Hudz, S., Zakomirnyi, D. (2025). Mathematical and graphical approaches to improve the process of saturation of flushing fluid with air in the circulation system of a drilling rig unit. Technology Audit and Production Reserves, 3 (1 (83)), 64–71. https://doi.org/10.15587/2706-5448.2025.329744

1. Introduction

The research considers an analogue of the well-known foam generating device [1], which was used during the development of wells. The disadvantage of this device is the unchanging geometric dimensions of the nozzle diameters and the lengths of the mixing chambers, which does not allow obtaining foam mixtures with a wide range of properties that are necessary during the development of oil and gas wells.

The main task of research is to improve the design of the foam generator to increase the efficiency of foam formation using a liquid and air mixer. This is the main reason why many manufacturers are looking for ways to improve the operation of circulation systems, for more efficient use of cleaning units, with minimal and reasonable costs. This topic was considered using the example of Ukrainian facilities, namely domestic scientists from oil and gas equipment [1, 2], studying the experience of scientists from other countries. Thus, in the paper [3] the authors, solving this problem, investigated how the geometric parameters of the foam generating device affect its operation. They analyze various design features and their impact on the efficiency of foam generation, which is important for optimizing well drilling processes.

Work [4] is devoted to increasing the efficiency of foam generating devices used in pumping and circulation systems of drilling rigs. The authors analyze existing designs and propose improvements to improve the performance and reliability of these systems.

The authors in work [5] conducted an experimental study of a new foam generator designed for drilling with reduced pressure. They evaluate its performance and efficiency in comparison with traditional methods, which can improve drilling processes under low pressure conditions. In work [6], the authors provide recommendations for the use of foaming surfactants.

In the work, the issue of improving the foam generator was solved by increasing the spectrum of properties of the foam mixture at the outlet without changing the pressure and fluid and air supply at the inlet to the foam generator. The design of the liquid and air mixer is made in such a way that it allows simultaneous supply of liquid and air to the pre-mixing chamber, where fields of developed turbulence are created in the working mixing zone. Such a technical solution makes it possible to increase the productivity of the device and its efficiency.

Fig. 1 shows the proposed design of the foam generator consisting of a cylindrical housing 1, in which a liquid and air mixer 2 with sealing rings 3 is placed. The pre-mixing chamber 4 is connected to a channel 5 for air supply, spacer rings 6, pressure rings 7, a foam mixture swirler 8, a diffuser 9 with a turbulent mixing chamber. Vertical holes 10 for liquid supply and horizontal 11 and vertical 12 holes for air supply are drilled in the liquid and air mixer.

The foam generator for saturating a liquid with air with subsequent foam formation works as follows. The liquid enters the housing 1 of the device and then through the holes 10 of the liquid and air mixer 2 into the pre-mixing chambers 4. Compressed air is simultaneously supplied to the mixer through the channel 5 in the housing 1 and openings 11 and 12 of the liquid and air mixer 2. After leaving the mixer, the air also enters the pre-mixing chambers 4, where fields of developed turbulence are created in the working mixing zone. In the mixing chambers from the spacer rings 6 and pressure rings 7, intensive turbulence of the jets occurs, air is mixed with the solution and foam is formed. The mixture then passes through the foam mixture swirler 8, which contributes to high-quality mixing and the formation of a foam mixture in the mixing chamber, which is placed in the diffuser 9, where the liquid moves in a turbulent mode and the effect of foam saturation with air is fixed.

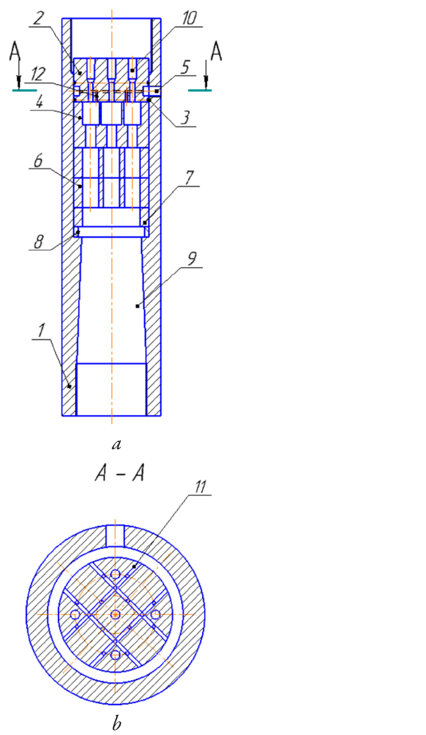

Fig. 1. ПГП-100x25-5 modernized multi-nozzle foam generator: *a* – longitudinal section; *b* – section along the plane A–A of the longitudinal section; 1 – housing; 2 – mixer; 3 – rings; 4 – pre-mixing chamber; 5 – channel; 6 – spacer rings; 7 – pressure rings; 8 – foam mixture swirler; 9 – diffuser; 10 – vertical holes; 11 – horizontal holes; 12 – air supply holes

Therefore, when implementing this design of a multi-nozzle foam generator equipped with a modernized mixing chamber, a high-quality aeration and foaming process is expected [7, 8]. Such a technical solution makes it possible to increase the productivity of the device [9] and the efficiency of the equipment.

The aim of research is to modernize a multi-nozzle foam generator. The task is solved using a new proposed design, namely an improved mixing chamber, which allows to increase the quality of the processes: foaming and aeration, as well as reduce the time spent on the well development process.

Modern requirements for the efficiency of drilling processes involve the use of technologies that provide high productivity and energy efficiency. One of the important components of such processes is foaming and high-quality aeration of the flushing fluid in the circulation systems of drilling rigs. Existing designs of foam generators often have limited efficiency of liquid saturation with air, which reduces the overall productivity of the equipment and increases the time spent on well development. Therefore, the task of improving the designs of foam generators is relevant in order to increase the efficiency of their operation.

Thus, *the aim of research* is to modernize the multi-nozzle foam generator by improving the design of the mixing chamber. The proposed technical solution allows to increase the efficiency of the foaming and aeration processes, ensure uniform saturation of the liquid with air, reduce energy losses and reduce the time required for well development, without changing the parameters of the air and liquid supply.

2. Materials and Methods

The object of research is the process of saturation of the flushing liquid with air using a multi-nozzle foam generator in the circulation systems of drilling rigs.

The study of the dynamics of the two-phase flow in the mixing chamber and the influence of geometric parameters and operating characteristics. A model with a central supply of liquid flowing from the nozzle is considered (Fig. 2). In this case, the air jet is supplied under pressure from the side channels of rectangular cross-section and in the mixing chamber is connected to the working fluid.

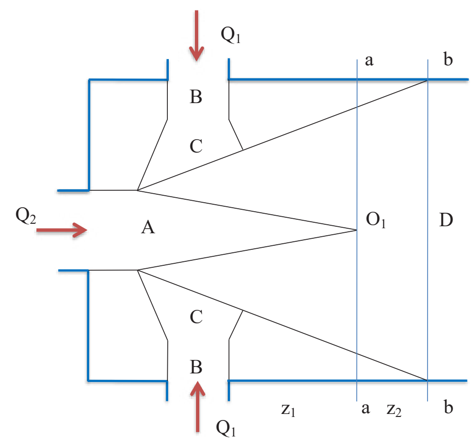

Fig. 2. Calculation scheme of the process of mixing flows

The working flow jet flowing out of the nozzle gradually expands due to the addition of air and at a certain distance from the inlet section of the mixing chamber (section *bb*) connects to its walls. As studies show, the boundaries of the jet are outlined by straight lines, and they have an unequal inclination to the axis in the sections of the mixing chamber Z_1 and Z_2. At the initial section of the mixing chamber in the central part of the jet there is a potential core A, the width of which decreases at a constant speed along the flow and at point O_1 takes zero values. The air flow moving in the chamber (region B) has the shape of a ring confuser. Between regions A and B, region C is formed, in which the two flows are mixed. In region D, the process of mixing the working fluid and air is completed. Depending on the geometric dimensions of the nozzles for supplying liquid and the channel for supplying air, point O_1 can be located (Fig. 2) to the right of section bb. In this case, the length of the section between sections *aa* and *bb* is $Z_2 = 0$.

In the model with a central liquid supply, a two-phase bubble flow flows along the axis, and in the peripheral zones – a droplet flow.

Let's assume a simplified one-dimensional scheme of two co-current flows in the mixing chamber at the initial and main sections: an air flow with a uniform velocity, temperature and density condenses on a liquid flow, which is also uniform in the cross section. Thus, the velocity, temperature and density of air and liquid are functions only of the longitudinal coordinate.

Let's carry out calculations under the following boundary assumptions:

1. The air flow does not contain moisture.
2. The liquid flow does not contain air bubbles.
3. The losses in the boundary layer on the wall are infinitely small.
4. The length of the initial and main sections is known and given by the experimental equation.
5. The mass of condensing air is added to the liquid at the air velocity.
6. The static pressure is constant in the cross section of the mixing chamber.

The results of the studies allow to conclude that their improvement will contribute not only to increasing the efficiency of drilling processes, but also to creating more economically profitable and environmentally safe technologies.

3. Results and Discussion

For the relative length of the initial section, the Lyshevskiy equation gives the best match with the experimental data

$$\frac{L}{d}=C_1 W_e^{-C_2}\left(\frac{\rho_1}{\rho_2}\right)^{C_3} L_p^{-C_4}, \tag{1}$$

where $C_1=50.3$, $C_2=0.83$, $C_4=0.096$; $W_e=p_1 d_1(\Delta\vartheta)^2/\sigma_2$ – Weber number; $\Delta\vartheta=\vartheta_3-\vartheta_1$; d_1, d_2 – diameters of air and liquid jets; σ_2 – surface tension of the liquid; μ_2 – viscosity of the liquid; ρ_1, ρ_2 – densities of air and liquid; $\vartheta_3-\vartheta_1$ – difference of phase velocities; $L_p=C_5\rho_2 d_2\sigma_2/\mu_2^2$ – Laplace criterion.

The length of the main section can be found from the experimental dependence

$$\frac{L}{D}=C_1 M_R^{-C_2}, \tag{2}$$

where M_R – dimensionless criterion characterizing the interaction of phases (momentum ratio). The length of the main section L is determined by the phase ratio, and the coefficients 18.36 and 0.181 are experimental; $C_1=18.36$, $C_2=0.181$; $M_R=\rho_2\vartheta_2/\rho_1\vartheta_1$ – ratio of the products of pressure and velocity of the liquid to the pressure and velocity of the air; D – diameter of the mixing chamber.

Let's write down the system of basic equations.

The equation of jet continuity:

– for air

$$\frac{d}{dz}\rho_1\varphi_0\vartheta_1 S_c=-\chi\varphi_{\max}S_k, \tag{3}$$

– for liquid

$$\rho_2\frac{d}{dz}(1-\varphi_0)\vartheta_2 S_c=\chi(1-\varphi_{\max})S_k, \tag{4}$$

where $\chi=dm_1/dt\cdot dV$ – condensation rate, i. e. the mass of air condensed per unit time per unit volume; $\chi=2\alpha''(T_s-T_2)\left(\sqrt{1-\varphi_{\max}}/\lambda R(z)\right)$ – here it is assumed that the air phase has a temperature equal to the saturation temperature T_s at $\rho=\text{const}$; α'' – heat transfer coefficient during condensation; $\varphi_{\max}$ – maximum value of vapor capacity at the exit from the main section of the mixing chamber; φ_0 – value of vapor capacity at the exit from the nozzle at the transition to the main section of the mixing chamber; S_k – cross-sectional area of the mixing chamber; S_c – areas of the inlet nozzles.

Change in the amount of movement:

– for the air phase

$$\rho_1\varphi_0\vartheta_1\frac{d\vartheta_1}{dz}=-F-\varphi_{\max}\frac{dp}{dz}, \tag{5}$$

– for the liquid phase

$$\rho_2(1-\varphi_0)\vartheta_2\frac{d\vartheta_2}{dz}+\chi(\vartheta_2-\vartheta_1)=F-(1-\varphi_{\max})\frac{dp}{dz}, \tag{6}$$

where F – friction force on the interface surface relative to the unit volume of the two-phase system;

$$F=\frac{C_f\rho_1(\vartheta_2-\vartheta_1)^2\sqrt{(1-\varphi_{\max})}}{R(z)}, \tag{7}$$

where $R(z)$ – radius of the mixing chamber; C_f – drag coefficient at the interface.

When air flows around a liquid stream near the nozzle cut, a laminar boundary layer is formed.

The drag coefficient in this zone is determined by the Blasius formula:

$$C_f=1.328\frac{1}{\sqrt{\text{Re}_z}}, \tag{8}$$

$$\text{Re}_z=\frac{\rho_1(\vartheta_2-\vartheta_1)z}{\mu_1}, \tag{9}$$

where μ_1 – dynamic viscosity of air.

At numbers greater than $5\cdot10^5$ the boundary layer becomes turbulent, in which the drag coefficient

$$C_f=0.0576\frac{1}{\sqrt[5]{\text{Re}_z}}. \tag{10}$$

Energy conservation equation for a thermally insulated chamber without taking into account friction on the walls:

– for the air phase

$$\rho_1\varphi_0\vartheta_1\frac{di_{01}}{dz}-\chi T_s s''(p)=\vartheta_1\varphi_{\max}\frac{dp}{dz}-F\vartheta_2-q_1, \tag{11}$$

– for the liquid phase

$$\rho_2(1-\varphi_0)\vartheta_2\frac{di_{02}}{dz}+\chi\left[i_{02}-i_{01}-T_s s'(p)\right]=$$
$$=\vartheta_2(1-\varphi_{\max})\frac{dp}{dz}+F\vartheta_2-\chi\lambda_1, \tag{12}$$

where q_1 – amount of heat transferred by convection from air to liquid, relative to unit volume;

– enthalpy of complete braking of the air phase

$$i_{01}=i_1+\frac{\vartheta_1^2}{2}, \tag{13}$$

– enthalpy of complete braking for the liquid

$$i_{02}=i_2+\frac{\vartheta_2^2}{2}, \tag{14}$$

where T_s – saturation temperature at a given pressure (depends on z); s'', s' – entropies of saturated air and liquid at a given pressure.

In the initial and main section of the chamber, q_1 can be approximately calculated taking into account forced convection on a longitudinally streamlined undeformed cylinder

$$q_1=\frac{\alpha'(T_s-T)_2\sqrt{(1-\varphi_{\max})}}{R(z)}. \tag{15}$$

Here it is assumed that the air phase has a temperature equal to the saturation temperature at $\rho=\text{const}$, and the liquid temperature is constant in the cross section. In reality, the temperature of the liquid layers of the liquid is lower, and at the surface it approaches the saturation temperature, so that the convective heat transfer from the air to the liquid, which is blocked by the heated surface layer on the jet surface, will become significantly lower.

The volumetric vapor capacity ϑ_0 is defined as the cross-sectional area of the mixing chamber occupied by air vapor in the nozzle cross section at $z=0$; the channel profile was given analytically as a function of z. For a conical chamber

$$S(z)=\pi\left(R_c-z\cdot\operatorname{tg}\beta\right)^2, \tag{16}$$

where β – half-opening angle of the mixing chamber; R_c – cut radius.

After the liquid jet was crushed at the cross section of the main chamber, a bubble or foam flow was formed. The input data for the analysis of this flow are the values obtained as a result of the numerical calculation of the system of equations (16).

It was assumed that the change in the structural flow is not accompanied by intensive condensation, i. e. the volumetric vapor capacity changes mainly due to the change in velocity when passing through the cross section of the main chamber.

To find the velocity of the homogeneous flow in the cross section of the main chamber, the momentum conservation equation is used

$$\vartheta''=x\vartheta_1'+(1-x)\vartheta_2', \tag{17}$$

where ϑ_1, ϑ_2 – velocities of the air and liquid phases in the cross section before the liquid jet breaks up.

The density and degree of dryness of the two-phase flow were determined from the continuity equations:

$$\rho_{int}=\frac{(m_1+m_2)}{\vartheta''_{int}S_{int}};x_{int}=\frac{m_1}{(m_1+m_2)}. \tag{18}$$

The initial vapor capacity φ_0 at the cross section was determined for $\rho_1/\rho_2\le 1$ as

$$\rho_{int}=(1-\varphi)\rho_2. \tag{19}$$

These equations allowed to establish the velocity, degree of dryness and vapor capacity at the entrance to the homogeneous section at the cross section. The mass, momentum and energy conservation equations for a bubble homogeneous flow have the following form.

The mass conservation equation

$$\frac{d\vartheta}{\vartheta}+\frac{dS}{S}+\frac{d\rho}{\rho}=0. \tag{20}$$

Differentiating equation (20)

$$\frac{d\rho}{\rho}=-\frac{d\varphi}{(1-\varphi)}, \tag{21}$$

and substituting the obtained equation into equation (20), let's obtain

$$\frac{d\vartheta}{\vartheta}=\frac{d\varphi}{(1-\varphi)}-\frac{dS}{S}. \tag{22}$$

The momentum conservation equation, taking into account the friction on the channel walls, has the form

$$dp=-\frac{(m_1+m_2)}{S}d\vartheta-\tau_w\frac{D}{S}dz, \tag{23}$$

where D – channel perimeter; τ_w – tangential stress on the walls.

Using equations (19) and (22), it is possible to find

$$\frac{dp}{dz}=-\frac{(m_1+m_2)^2}{S^2(1-\varphi)\rho_2}\left\{-\frac{1}{S}\frac{dS}{dz}+\frac{1}{1-\varphi}\frac{d\varphi}{dz}\right\}-\tau_w\frac{D}{S}. \tag{24}$$

For a conical mixing chamber there is the system

$$\begin{cases}\dfrac{1}{S}\cdot\dfrac{dS}{dz}=-\dfrac{\operatorname{tg}\beta}{2\left(R_c-z\cdot\operatorname{tg}\beta\right)};\\[2ex] \dfrac{dp}{dz}=-\dfrac{(m_1+m_2)^2}{S^2(1-\varphi)\rho_2}\left\{-\dfrac{\operatorname{tg}\beta}{2\left(R_c-z\cdot\operatorname{tg}\beta\right)}+\dfrac{1}{1-\varphi}\cdot\dfrac{d\varphi}{dz}\right\}-\tau_w\dfrac{D}{S}.\end{cases} \tag{25}$$

Additional equations of the relationship between ρ, x and ϑ were found from the relation for the density of the substance, namely

$$\rho x=\rho_1\varphi \text{ and } \rho(1-x)=\rho_2(1-\varphi). \tag{26}$$

Dividing the first equation by the second, it is possible to obtain

$$\frac{x}{1-x}=\frac{\varphi}{1-\varphi}\cdot\frac{\rho_1}{\rho_2}. \tag{27}$$

Differentiating (27) it is possible to obtain

$$\frac{dx}{x(1-x)}=\frac{d\varphi}{(1-\varphi)\varphi}+\frac{d\rho_1}{\rho_1}. \tag{28}$$

Using the polytrope equation for the vapor phase in diff. form

$$\frac{dp}{np}=\frac{d\rho_1}{\rho_1}, \tag{29}$$

and substituting it into equation (28) let's obtain an equation that relates pressure, dryness and vapor capacity in the following form

$$\frac{dx}{x(1-x)}=\frac{d\varphi}{(1-\varphi)\varphi}+\frac{dp}{np}. \tag{30}$$

The left-hand side of this equation expresses the rate of relative change of the air phase and can be determined using the heat balance equation

$$\lambda dm_1=-\alpha(T_1-T_2)S, \tag{31}$$

or

$$\lambda dx=-\frac{\alpha(T_1-T_2)S}{m_1+m_2}, \tag{32}$$

where α – heat transfer coefficient during condensation, $S/(m_1+m_2)$ – surface area of the bubbles in a given cross section relative to the mass flow rate of the two-phase medium.

Let's express the surface $S/(m_1+m_2)$ in terms of the number of bubbles currently in the intersection

$$\frac{S}{m_1+m_2}=\frac{N\pi d^2}{m_1+m_2}=\frac{6x}{\rho_1 d}\frac{dz}{\vartheta}=\frac{3x}{d/2}\frac{1}{\rho_1\vartheta}dz, \tag{33}$$

or

$$\frac{dx}{x}=-\frac{3\alpha(T_1-T_2)}{\lambda(d/2)\rho_1\vartheta}dz. \tag{34}$$

 ISSN-L 2664-9969; E-ISSN 2706-5448

Expressing the air density from the polytropic equation and substituting (34) into (31), it is possible to obtain approximately

$$\frac{dp}{np}=-\frac{d\varphi}{(1-\varphi)\varphi}-\frac{3\alpha(T_1-T_2)}{\lambda\left(\frac{d}{2}\right)\rho_{1int}\left(\frac{p}{p_{int}}\right)^{1/n}\vartheta}dz. \tag{35}$$

Equations (25) and (35) express the dependence of pressure on the volumetric vapor capacity and the passage channel. Combining these equations

$$\frac{dp}{dz}=-\frac{(m_1+m_2)^2}{S^2(1-\varphi)\rho_2}\cdot\frac{1}{S}\frac{dS}{dz}+$$
$$+\frac{(m_1+m_2)^2\varphi}{S^2(1-\varphi)\rho_2 n}\cdot\frac{dp}{pdz}-L_Q\varphi-\tau_w\frac{D}{S}\cdot\frac{(m_1+m_2)^2}{S^2(1-\varphi)\rho_2}, \tag{36}$$

where $L_Q=\frac{3\alpha(T_1-T_2)}{\lambda\left(\frac{d}{2}\right)\rho_{1int}\left(\frac{p}{p_{int}}\right)^{1/n}\vartheta}$ – heat multiplier, or in this form

$$\frac{dp}{dz}=-\frac{\frac{(m_1+m_2)^2}{S^2(1-\varphi)\rho_2}\left[\frac{1}{S}\cdot\frac{dS}{dz}+L_Q-\tau_w\frac{D}{S}\right]}{1-\frac{(m_1+m_2)^2\varphi}{S^2(1-\varphi)\rho_2 np}}. \tag{37}$$

The speed of sound in a two-phase bubble medium in the absence of phase changes has the form

$$a=\left[\frac{np}{\varphi(1-\varphi)\rho_2}\right]^{1/2}. \tag{38}$$

Then the last equation of the influence on pressure will be

$$\frac{dp}{dz}=-\frac{\vartheta^2\rho\left[\frac{1}{S}\cdot\frac{dS}{dz}+L_Q-\tau_w\frac{D}{S}\right]}{1-M^2}, \tag{39}$$

where M – Mach number, which is calculated at the speed of sound for a two-component medium.

Integrating (39) using the Maple 9.5 program, it is possible to obtain an equation that determines the relationship between the pressure of the mixture at the outlet of the mixing chamber and its length

$$p(Z)=-C_3e^{\frac{\vartheta^2\rho\left[1+L_QS-\pi\cdot\tau_wD\right]l_2}{S(M-1)(M+1)}}, \tag{40}$$

where l_2 – length of the main section of the mixing chamber.

The coefficient C_3 is determined from the condition that at the entrance to the mixing chamber of the ejection-type device $l_2=0$, and therefore $\rho(0)=-C_3$ and therefore $C_3=-\rho_2(z)$.

With a determined coefficient C_3, equation (40) makes it possible to predict the pressure level of the foam mixture at the stage of preliminary calculation and selection of the main equipment for drilling wells using foam. This prediction occurs at the outlet of the ejection-type device with a certain length of the mixing chamber.

The length of the mixing chamber of the liquid-air mixer directly affects its parameters. To obtain maximum efficiency, a rational choice of the length of the mixing chamber is important [10].

The length of the mixing chamber was determined by the formula

$$L_k=l_1+l_2, \tag{41}$$

where l_1 – length of the initial section of the mixing chamber; l_2 – length of the main section of the mixing chamber.

To determine the length of the initial section of the mixing chamber, it is possible to use the formula

$$l_1=Z_1+Z_2. \tag{42}$$

The relative length of the initial section of the working jet in the mixing chamber of the ejection-type device was determined by the formula

$$\frac{Z_1}{D}=\frac{4.188}{K_{mc}^{0.5}}\left[1-0.379\left(1-\frac{1.032u}{K_{mc}-1}\right)\right], \tag{43}$$

where u – ejection coefficient; K_{mc} – geometric parameter of the mixing chamber of the ejection-type device, determined by the formula

$$K_{mc}=\frac{S}{S_2}, \tag{44}$$

where S – cross-sectional area of the mixing chamber; S_2 – cross-sectional area of the nozzle for supplying liquid.

The relative length of the section of the mixing chamber, in the final cross-section of which the boundaries of the working jet were connected to its walls, was determined by the formula

$$\frac{Z_2}{D}=$$
$$=\frac{0.232\left(1-3.278K_{mc}^{-1}\right)\left[1+2.893u\left(K_{mc}-1\right)^{-1}\ln\left(0.305K_{mc}^{0.5}\right)\right]}{K_{mc}^{0.5}\ln\left[\frac{1+u}{0.257K_{mc}}-\frac{2.891u}{K_{mc}-1}\right]^{-1}}. \tag{45}$$

For the relative length of the main section, the experimental dependence gives a better match with the experimental data

$$\ln\left(\frac{l_2}{D}\right)=\ln(18.36)-0.181\ln M_R, \tag{46}$$

where M_R – ratio of the air momentum at the nozzle outlet to the fluid momentum, determined by the formula

$$M_R=\left(\frac{\rho_2}{\rho_1}\right)\left(\frac{\upsilon_2}{\upsilon_1}\right)^2, \tag{47}$$

where ρ_2/ρ_1 – density ratio; $(\upsilon_2/\upsilon_1)^2$ – square of the velocity ratio.

The results of calculations in the Maple 9.5 software package for each operating mode of the mud pump and different diameters of the holes of the multi-nozzle ejection type inserts are shown in Fig. 3–8.

So, for the graphs (Fig. 3–8) the regularity of increasing the air flow rate is characteristic in proportion to the increase in its supply pressure and liquid flow rate. The fact of the presence of the phenomenon of "separation" of the curves for values of 0.2 MPa from another array of the obtained graphs is of interest. Such a phenomenon is characteristic of the graphical dependencies shown in Fig. 4, 6. This opens up avenues for further research of the developed equipment in the direction of optimizing its operating parameters [11–13].

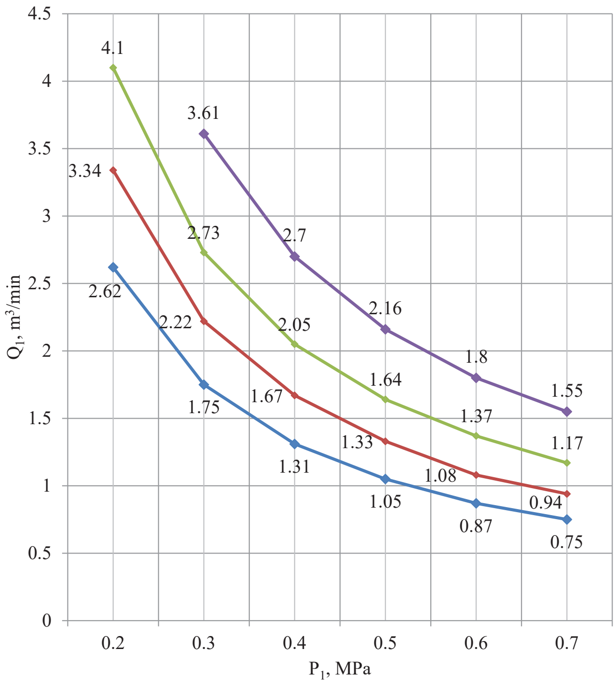

Fig. 3. Dependence of air flow rate on its pressure at $d_c=4$ mm: 1st row – $P_2=13$ MPa; $Q_2=8.8\cdot10^{-3}$ m³/s; 2nd row – $P_2=10$ MPa; $Q_2=11.20\cdot10^{-3}$ m³/s; 3rd row – $P_2=8$ MPa; $Q_2=13.75\cdot10^{-3}$ m³/s; 4th row – $P_2=6$ MPa; $Q_2=18.15\cdot10^{-3}$ m³/s

1 row; 2 row; 3 row; 4 row

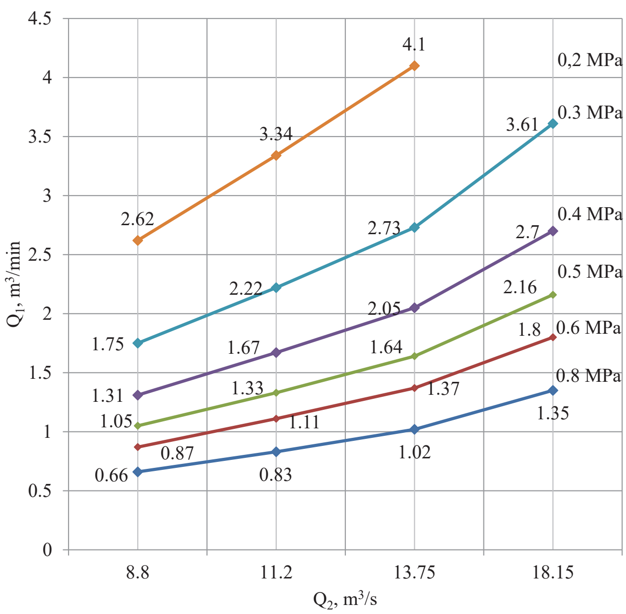

Fig. 4. Dependence of air flow rate on liquid flow rate at $d_c=4$ mm

Practical significance. The mechanism of foam formation and operational characteristics, which take into account the flow of liquid through the nozzle and gas from the supply pipe to the foam generating device, demonstrate the interaction of these flows. Due to turbulent transverse velocity pulsations, liquid dispersion occurs in the transverse direction and the jet is aerated by air.

Subsequently, its decomposition into an air-droplet mixture, the formation of an air-droplet homogeneous flow and its movement to the seal jump occur. The jump is accompanied by the transformation of the air-droplet mixture into a liquid-bubble mixture, in which the air bubbles have approximately the same diameter and are separated by liquid films. To obtain a compaction jump, it is necessary that the speed of the air-droplet flow exceeds the speed of sound in it. Given this, the practical significance of the research is that the geometric shapes, dimensions of the foam generator components, as well as modes and parameters are decisive for the efficiency of its operation.

Research limitations. It has been theoretically established that with a gas (air) content of 20–80% in a liquid (water) with surfactants, for the formation of fine foam, the flow velocity of the mixture before the compaction jump should reach 30–40 m/s. In the case when the gas content is 80–95%, the required speed increases to 40–60 m/s. When the liquid flow rate increases above the set limit, the foaming efficiency decreases, since the flow speed before the compression jump increases and the Mach number increases accordingly.

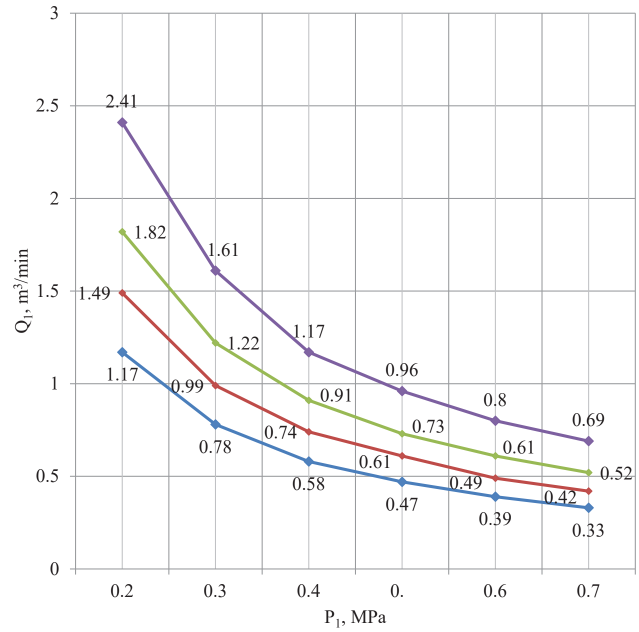

Fig. 5. Dependence of air flow rate on its pressure at $d_c=6$ mm: 1st row – $P_2=13$ MPa; $Q_2=8.8\cdot10^{-3}$ m³/s; 2nd row – $P_2=10$ MPa; $Q_2=11.20\cdot10^{-3}$ m³/s; 3rd row – $P_2=8$ MPa; $Q_2=13.75\cdot10^{-3}$ m³/s; 4th row – $P_2=6$ MPa; $Q_2=18.15\cdot10^{-3}$ m³/s

1 row; 2 row; 3 row; 4 row

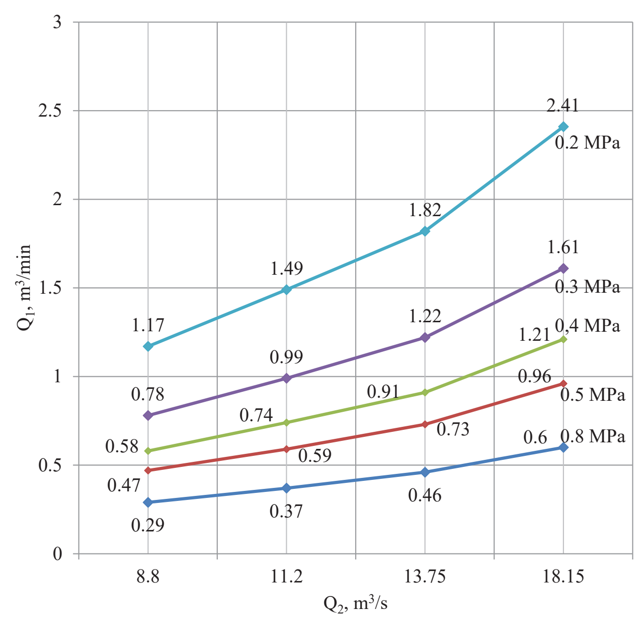

Fig. 6. Dependence of air flow rate on liquid flow rate at $d_c=6$ mm

ISSN-L 2664-9969; E-ISSN 2706-5448

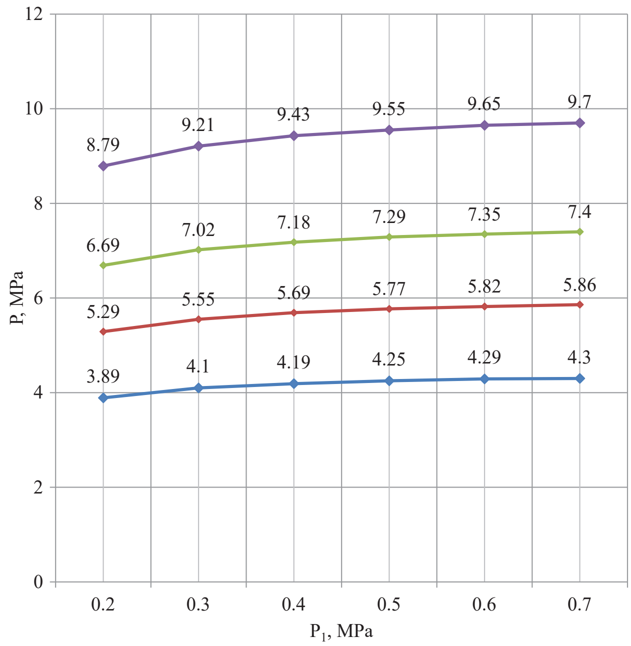

Fig. 7. The value of the foam pressure at the outlet of the ejection type device for the pump operating mode at the highest flow rate: 1 row – $P_2=13$ MPa; $Q_2=8.8\cdot10^{-3}$ m^3/s; 2 row – $P_2=10$ MPa; $Q_2=11.20\cdot10^{-3}$ m^3/s; 3 row – $P_2=8$ MPa; $Q_2=13.75\cdot10^{-3}$ m^3/s; 4 row – $P_2=6$ MPa; $Q_2=18.15\cdot10^{-3}$ m^3/s
1 row; 2 row; 3 row; 4 row

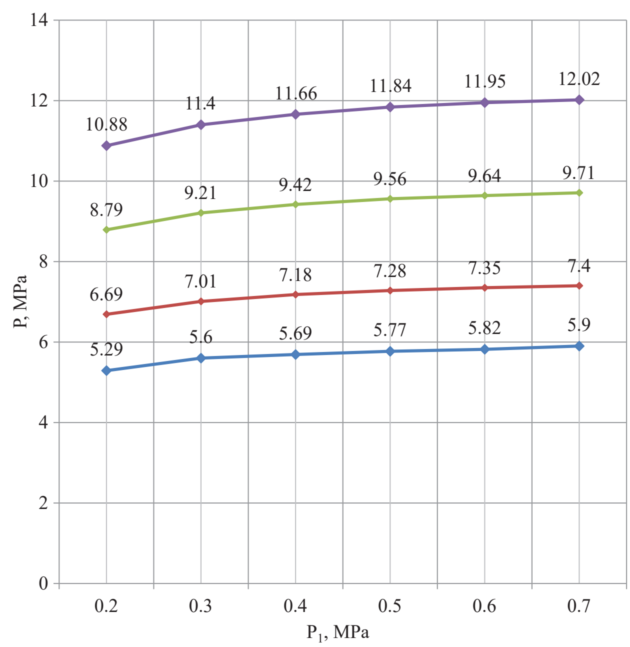

Fig. 8. The value of the foam pressure at the outlet of the ejection type device for the pump operating mode at the highest pressure: 1 row – $P_2=16$ MPa; $Q_2=6.49\cdot10^{-3}$ m^3/s; 2 row – $P_2=13$ MPa; $Q_2=8.25\cdot10^{-3}$ m^3/s; 3 row – $P_2=10$ MPa; $Q_2=10.15\cdot10^{-3}$ m^3/s; 4 row – $P_2=8$ MPa; $Q_2=13.37\cdot10^{-3}$ m^3/s
1 row; 2 row; 3 row; 4 row

Prospects for further research. To continue theoretical studies of the foaming process, it is planned to conduct computer modeling. This will allow a deeper study of the processes occurring during the movement of liquid, gas and gas-liquid mixture flows along the foam generator, in comparison with experimental studies. In the future, experimental studies of the foam generator with optimal geometric dimensions will be conducted.

4. Conclusions

The conducted research of the processes of mixing flows in the mixing chamber of the ejection-type device allowed to identify key patterns that determine the efficiency of the system. Analysis of the geometric parameters of the mixing chamber, as well as the dependences of the air flow rate on the pressure and liquid flow rate, showed that the efficiency of the process is significantly affected by the ratio between the parameters of the air and liquid supply, as well as the design features of the nozzles and the mixing chamber.

It was established that the air flow rate increases proportionally to the increase in its supply pressure, and the liquid flow rate determines the nature of the flow distribution in the chamber. The presence of a "separation" of the curves at low air pressure values (0.2 MPa) indicates a complex interaction of flows in certain operating modes, which opens up prospects for further study of the process and improvement of the design parameters of the system.

Experimental dependencies confirmed that the length of the mixing chamber is a critical parameter for achieving the optimal coefficient of performance (efficiency) of the system. The rational choice of the length of the initial and main sections of the mixing chamber allows to significantly improve the mixing performance of the flows, ensuring uniform pressure distribution and reducing energy losses.

The results of calculations in the software environment "Maple 9.5" showed that the foam pressure at the outlet of the mixing chamber depends on the geometry of the device, the operating modes of the pump and the diameter of the nozzles. This confirms the importance of integrating numerical modeling methods for predicting the parameters of the system at the design stage.

The results obtained open up new opportunities for optimizing the operating characteristics of ejection-type devices. Improving the design and operating parameters will increase the efficiency of their use in drilling rigs, reduce energy costs, and also ensure a high level of environmental safety due to accurate prediction of the parameters of the two-phase flow at the outlet.

Conflict of interest

The authors declare that they have no conflict of interest in relation to this research, whether financial, personal, authorship or otherwise, that could affect the research and its results presented in this paper.

Financing

The research was performed without financial support.

Data availability

The manuscript has no associated data.

Use of artificial intelligence

The authors used artificial intelligence technologies within acceptable limits to provide their own verified data, which is described in the research methodology section.

References

1. Savyk, V. M., Liakh, M. M., Mykhailiuk, V. V. (2013). Pat. No. 77955 UA. *Pinoheneruiuchyi prystrii bahatosoplovyi.* MPK V01F 3/04, E02V 8/00. No. u201205435; declareted: 03.05.12; published: 11.03.13. Bul. No. 5, 6.
2. Liakh, M. M., Savyk, V. M., Molchanov, P. O. (2017). Experimental and industrial research on foamgenerating devices. *Naukovyi Visnyk Natsionalnoho Hirnychoho Universytetu, 5 (161),* 17–23. Available at: https://nvngu.in.ua/index.php/uk/arkhiv-zhurnalu/za-vipuskami/1493-2017-ukr/zmist-5-2017/

rozrobka-rodovishch-korisnikh-kopalin/4151-eksperimentalni-ta-promislovi-doslidzhennya-pinogeneruyuchikh-pristrojiv

3. Kuzmenko, V. P., Lysenko, O. M. (2012). Otsinka vplyvu heometrychnykh parametriv na robotu pinoheneruiuchoho prystroiu. *Rozvidka ta rozrobka naftovykh i hazovykh rodovyshch, 2 (43),* 123–130. Available at: https://irbis-nbuv.gov.ua/cgi-bin/irbis_nbuv/cgiirbis_64.exe?C21COM=2&I21DBN=UJRN&IMAGE_FILE_DOWNLOAD=1&Image_file_name=PDF%2Frrngr_2012_2_23.pdf&P21DBN=UJRN
4. Petrenko, I. V., Sydorenko, R. M. (2016). Improving the efficiency of foamgenerating devices of pump-circulative systems of drilling sets. *Naukovyi visnyk NHU, 3,* 56–63. Available at: https://mail.nvngu.in.ua/index.php/uk/arkhiv-zhurnalu/za-vipuskami/1247-2016/zmist-3-2016/rozrobka-rodovishch-korisnikh-kopalin/3517-pidvishchennya-efektivnosti-pinogeneruyuchikh-pristrojiv-nasosno-tsirkulyatsijnikh-sistem-burovikh-ustanovok
5. Cao, P., Chen, Z., Liu, M., Cao, H., Chen, B. (2019). Numerical and experimental study of a novel aerodynamic foam breaker for foam drilling fluid. *Energy Science & Engineering, 7 (6),* 2410–2420. https://doi.org/10.1002/ese3.428
6. Shendrik, O., Fyk, M., Biletskyi, V., Kryvulia, S., Donskyi, D., Alajmeen, A., Pokhylko, A. (2019). Energy-saving intensification of gas-condensate field production in the east of Ukraine using foaming reagents. *Mining of Mineral Deposits, 13 (2),* 82–90. https://doi.org/10.33271/mining13.02.082
7. Liakh, M. M., Savyk, V. M., Molchanov, P. O. (2016). Improving the efficiency of foam-generating devices of pump-circulative systems of drilling sets. *Naukovyi Visnyk Natsionalnoho Hirnychoho Universytetu, 3,* 16–23. Available at: https://nvngu.in.ua/index.php/uk/arkhiv-zhurnalu/za-vipuskami/1247-2016/zmist-3-2016/rozrobka-rodovishch-korisnikh-kopalin/3517-pidvishchennya-efektivnosti-pinogeneruyuchikh-pristrojiv-nasosno-tsirkulyatsijnikh-sistem-burovikh-ustanovok
8. Krot, O. Yu., Korobko, B. O., Krot, O. P., Virchenko, V. V. (2023). *Eksperymentalni metody doslidzhen.* Poltava: NUPP, 192.
9. Syvko, V. Ya., Skubok, Ye. O. (1998). Rukh dynamichnoi systemy z urakhuvanniam vnutrishnoho oporu seredovyshcha. *Zbirnyk naukovykh prats "Vibrotekhnolohiia – 98". Obrobka dyspersnykh materialiv i seredovyshch. Teoriia, doslidzhennia. Tekhnolohiia ta obladnannia.* Kyiv: NVO "VOTUM", 16–21.
10. Kaliuzhnyi, A., Molchanov, P., Savyk, V., Knysh, M., Yaremiychuk, R. (2022). Determining foaming regularities enabled by a five-nozzle foam generator for drilling technologies under conditions of abnormally low pressures. *Eastern-European Journal of Enterprise Technologies, 4 (1 (118)),* 72–79. https://doi.org/10.15587/1729-4061.2022.262506
11. Lu, C., Wu, Y., Zhu, D., Liang, Y. (2024). *Study on the foam production characteristics of air self-suction foam generator by jet.* https://doi.org/10.21203/rs.3.rs-4804887/v1
12. Li, D., Li, F., Deng, S., Liu, J., Huang, Y., Yang, S. (2022). Preparation of Oil-Based Foam Gel with Nano-SiO_2 as Foam Stabilizer and Evaluation of Its Performance as a Plugging Agent for Fractured Shale. *Geofluids, 2022,* 1–12. https://doi.org/10.1155/2022/9539999
13. Al-Darweesh, J., Aljawad, M. S., Al-Ramadan, M., Elkatatny, S., Mahmoud, M., Patil, S. (2022). Review of underbalanced drilling techniques highlighting the advancement of foamed drilling fluids. *Journal of Petroleum Exploration and Production Technology, 13 (4),* 929–958. https://doi.org/10.1007/s13202-022-01596-w

✉ ***Petro Molchanov,*** *PhD, Associate Professor, Department of Professional Education and Design, Poltava V. G. Korolenko National Pedagogical University, Poltava, Ukraine, e-mail: petja_men@ukr.net, ORCID: https://orcid.org/0000-0001-5335-4281*

Tetiana Surzhko, *PhD Student, Department of Oil and Gas Engineering and Technology, National University "Yuri Kondratyuk Poltava Polytechnic", Poltava, Ukraine, ORCID: https://orcid.org/0000-0001-8095-3984*

Maksym Knysh, *PhD Student, Department of Oil and Gas Engineering and Technology, National University "Yuri Kondratyuk Poltava Polytechnic", Poltava, Ukraine, ORCID: https://orcid.org/0000-0002-3516-4852*

Yuliya Sribna, *PhD, Associate Professor, Department of Theory and Methods of Technological Education, Poltava V. G. Korolenko National Pedagogical University, Poltava, Ukraine, ORCID: https://orcid.org/0000-0003-3846-3871*

Vasyl Savyk, *PhD, Associate Professor, Department of Oil and Gas Engineering and Technology, National University "Yuri Kondratyuk Poltava Polytechnic", Poltava, Ukraine, ORCID: https://orcid.org/0000-0002-0706-0589*

Serhii Novopysmennyi, *PhD, Associate Professor, Department of Biology, Human Health and Physical Rehabilitation, Poltava V. G. Korolenko National Pedagogical University, Poltava, Ukraine, ORCID: https://orcid.org/0000-0003-1484-7918*

Oleksii Debre, *PhD, Assistant, Department of Theory and Methods of Technological Education, Poltava V. G. Korolenko National Pedagogical University, Poltava, Ukraine, ORCID: https://orcid.org/0000-0001-5174-6492*

Yuliia Salenko, *Doctor of Technical Sciences, Professor, Department of Machinery Engineering, Kremenchuk Mykhailo Ostrohradskyi National University, Kremenchuk, Ukraine, ORCID: https://orcid.org/0000-0002-5458-0990*

Serhii Hudz, *PhD, Associate Professor, Department of Architecture, Pryazovskyi State Technical University, Dnipro, Ukraine, ORCID: https://orcid.org/0000-0002-4764-8635*

Dmytro Zakomirnyi, *PhD Student, Department of Construction and Civil Engineering, National University "Yuri Kondratyuk Poltava Polytechnic", Poltava, Ukraine, ORCID: https://orcid.org/0009-0005-9803-0324*

✉ *Corresponding author*